THERMOECONOMIC ANALYSIS OF A SOLAR-DRIVEN HIGH-TEMPERATURE ELECTROLYSIS PLANT FOR HYDROGEN PRODUCTION IN BRAZIL

Diego Luis Izidoro[1,2]*, Silvio de Oliveira Junior[2]

[1]Federal Institute of Education, Science and Technology of Minas Gerais (IFMG), Formiga, Minas Gerais, Brazil

[2]Polytechnic School, Mechanical Engineering Department, University of São Paulo, São Paulo, São Paulo, Brazil

*Corresponding Author: diego.izidoro@ifmg.edu.br

ABSTRACT

Hydrogen is recognized as a key solution for decarbonizing various sectors, but its current production is mainly from fossil fuels. Developing alternative hydrogen production methods from renewable sources is crucial for its large-scale adoption. This study aims to perform a thermoeconomic analysis of a new proposed arrangement for a high-temperature electrolysis (HTE) plant powered by solar energy for large-scale hydrogen production. The plant is modeled using solid oxide electrolyzer cells (SOEC) and is designed for operation on the northeast coast of Brazil. The analysis is based on a 100 MW-SOEC plant consisting of 20 modules with a capacity of 5 MW each, with a photovoltaic (PV) system for electricity supply and a concentrated solar thermal (CST) system with thermal energy storage for steam production. Exergy analysis is performed at the thermoneutral voltage of the electrolyzers, and a thermoeconomic analysis evaluates the costs of renewable hydrogen production. For the proposed plant, the exergy efficiency is 15.6%, and the levelized cost of hydrogen (LCOH) is 3.63 US$/kg for a long-term scenario. These findings indicate higher efficiency than other renewable hydrogen production methods and suggest that, despite current high costs, the proposed plant is expected to become competitive with technological advancements and cost reductions in electrolyzers and equipment.

1 INTRODUCTION

The global need for sustainable and renewable energy sources has intensified the exploration of solar energy and hydrogen as promising alternatives for a greener energy matrix. Solar energy, with its abundant availability and low environmental impact, offers a viable solution through photovoltaic (PV) systems for electricity generation and concentrating solar thermal (CST) systems for electricity and heating. Specifically, CST plants leverage heliostats to concentrate solar radiation, enabling the production of steam and the potential for thermal storage, thereby ensuring continuous energy supply even during cloudy periods or for a limited time at night, depending on the storage capacity (Pourasl et al., 2023). Hydrogen, on the other hand, is emerging as an essential energy carrier for achieving decarbonization, especially in sectors where direct electrification poses challenges (Capurso et al., 2022). Its wide-ranging applications in the chemical industry, and it has the potential to be the most cost-effective low-carbon alternative for more than twenty different applications, including long-distance transportation, urban vehicles, trains, the steel industry, energy storage, and residential heating (Abdin et al., 2020).

The production of hydrogen from renewable sources, such as solar energy, is gaining traction as a means to further reduce the environmental impact of hydrogen production, which has traditionally been dominated by fossil fuel-based pathways (Younas et al., 2022). Electrolysis is the most advanced and sustainable method using renewable electricity, resulting in what is known as “green hydrogen” (Squadrito et al., 2023). High-temperature electrolysis (HTE) using solid oxide electrolysis cells (SOECs) offers higher efficiencies and faster chemical kinetics compared to the conventional process, resulting in reduced energy losses (O’Brien, 2012). SOECs have excellent operating flexibility. These

https://doi.org/10.52202/077185-0044

cells can directly convert steam, carbon dioxide, or both into hydrogen or syngas, respectively. They can also be integrated with different chemical synthesis processes, enabling the recycling of H_2O and captured CO_2 into synthetic fuels like methane, methanol, ammonia, and others. Moreover, when operated in reverse, the electrolyzer cell acts as a solid oxide fuel cell (SOFC) (Hauch et al., 2020).

The integration of HTE with solar energy, especially CST for electrical and thermal supply, has been investigated for a range of concentration technologies. Recent studies, including those by Restrepo et al. (2022) and Nejadian et al. (2023), have proposed hybrid configurations combining photovoltaic (PV) and concentrated solar thermal (CST) systems. These configurations have presented economic advantages, mainly due to the declining costs of PV systems. However, many technical and economic aspects still need further exploration for these types of plants, including operating strategies and conditions, site selection, heat recovery, energy storage, and integration with chemical synthesis processes. Therefore, this study presents a novel and highly efficient configuration of a solar-driven HTE plant for large-scale hydrogen production, integrating concentrating solar thermal (CST) technology for steam generation with photovoltaics (PV) for electricity supply. It conducts a comprehensive exergy and thermoeconomic assessment to evaluate the plant's efficiency and the levelized cost of hydrogen (LCOH). Furthermore, the analysis focuses on the Brazilian scenario, specifically in Pecém, on the northeast coast of the country, a region with high solar resource availability and industrial and port infrastructure.

2 METHOD

2.1 SOEC System Model

In this study, the analysis was conducted using a semi-empirical model of a SOEC system according to the papers of O'Brien (2012), Petipas et al. (2013), and Hansen (2015). The simulation was carried out considering operation at a thermoneutral voltage (V_{TN}), which is defined by Equation (1) as a function of the enthalpy of the electrolysis reaction (ΔH).

$$V_{TN} = \frac{\Delta H}{2F} \tag{1}$$

The irreversible losses in the SOEC stacks can be represented by the Area Specific Resistance (ASR), which varies with the operating temperature (T) and is estimated using the empirical correlation presented in Equation (2). The coefficient ε is used to adjust the curve and obtain the accurate ASR for the electrolyzer. In the case of a stack configuration, ε can be assumed to be 0.25 Ω·cm², while for a single cell, ε is close to zero (Fu et al., 2010).

$$ASR = exp\left(\frac{4900}{T} - 5.95\right) + \varepsilon \tag{2}$$

The stack current density (j), in A/cm², is calculated by Equation (3), where V represents the operating voltage and V_N is the Nernst open-cell potential.

$$j = \frac{V - V_N}{ASR} \tag{3}$$

The Nernst potential (V_N), determined using Equation (4), accounts for the minimum voltage required for the electrolysis process, considering the range of gas compositions encountered in real cells. The Nernst voltage depends on the average temperature (T) and pressure (p) of the reaction, and the average partial pressures of the involved gases (p_{H_2}, p_{O_2}, and p_{H_2O}). Here, ΔG denotes the change in Gibbs free energy, R is the universal gas constant, F is the Faraday constant, and p_0 refers to the pressure at standard conditions.

https://doi.org/10.52202/077185-0044

$$V_N = \frac{\Delta G + RT}{2F} ln\left(\sqrt{\frac{p}{p_0}} \cdot \frac{p_{H_2}\sqrt{p_{O_2}}}{p_{H_2O}}\right) \quad (4)$$

The total area of the SOEC stacks (A_{SOEC}) is calculated using Faraday's Law, as expressed in Equation (5), based on the required hydrogen molar flow rate ($\dot{n}_{H_2}$). Finally, Equation (6) gives the electrical power ($\dot{W}_{SOEC}$) needed for the electrolysis.

$$A_{SOEC} = \dot{n}_{H_2} \frac{2F}{j} \quad (5)$$

$$\dot{W}_{SOEC} = V \cdot j \cdot A_{SOEC} \quad (6)$$

2.2 Proposed plant description

The proposed arrangement is illustrated in Figure 1. It was designed to achieve higher efficiency and lower hydrogen production costs than previously proposed configurations. The plant comprises 100 MW of electrolyzers integrated with CST and PV systems. The CST includes a field of heliostats, a solar tower, and thermal energy storage (TES) tanks filled with solar salt, providing the necessary heat for steam generation. The PV system supplies electricity, with a grid connection also considered for exporting/importing electricity depending on the plant's demand. An enhanced heat exchanger network recovers exergy from the gas streams exiting the electrolyzer. The SOEC stacks operate at a thermoneutral voltage to maintain a constant temperature, using steam as the sweep gas in the anode for oxygen separation. Hydrogen and oxygen are separated, compressed, and stored at high pressure. Additionally, the plant recovers low-grade energy from gases in compression intercoolers to generate hot water for facility applications.

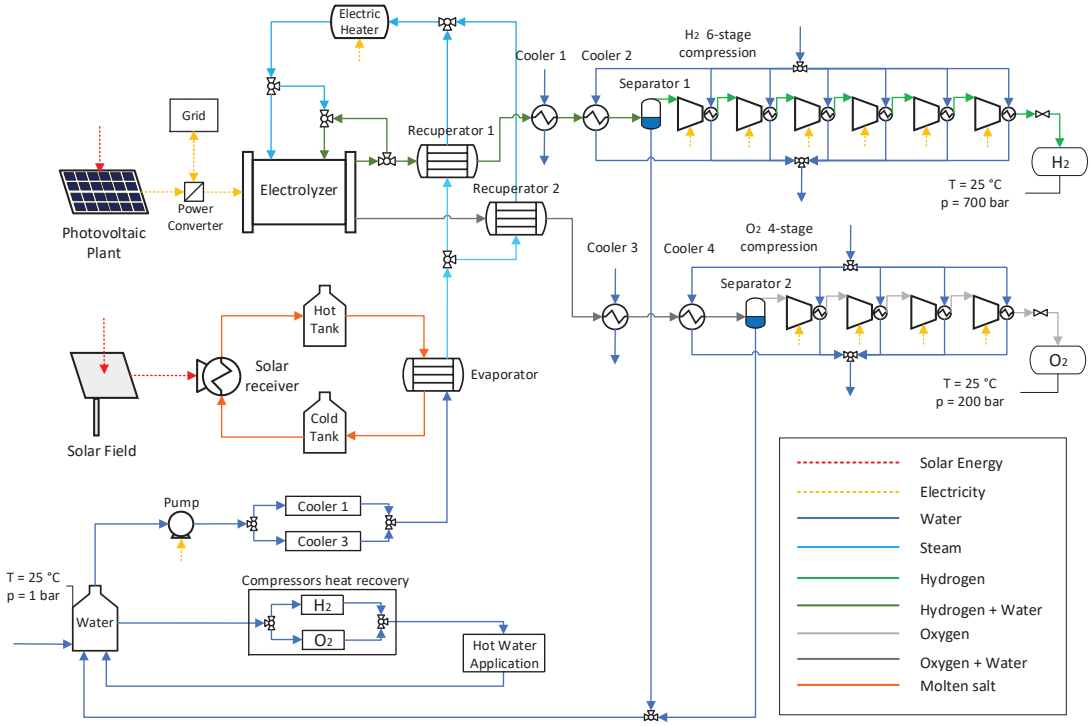

Figure 1: Proposed plant for hydrogen production

https://doi.org/10.52202/077185-0044

The plant was modeled in Python, using the PySAM package for the CST and PV systems (NREL 2024) and CoolProp library to obtain the thermophysical properties of substances (Bell et al., 2014). The study was carried out for Pecém, a coastal district in north-eastern Brazil, based on data from the National Solar Radiation Database (Sengupta et al., 2018) considering a typical meteorological year (TMY). The following operating conditions are considered:

- SOEC: 20 modules of 5 MW each, operating at 800°C and 10 bar, with a 75% steam molar conversion rate.
- CST: Solar multiple of 2.0 and 8 hours of full-load thermal storage.
- PV: Module energy efficiency of 19% and power conversion efficiency of 85%.
- Grid: balances energy demand and supply by receiving surplus electricity or providing additional electricity when necessary.
- Heat exchangers: Pinch points of 10 K and 15 K for gas/liquid and gas/gas exchangers, respectively, and a 40 mbar pressure drop.
- Pumps and compressors: Isentropic efficiency of 85% and electromechanical efficiency of 95%, respectively.
- Gas storage: Hydrogen at 700 bar and oxygen at 200 bar.

2.3 Exergy and Thermoeconomic Analysis

The exergy efficiency of electrolyzers can be calculated as the ratio of the total exergy rate of the products ($\dot{B}_{prod}$) to the input exergy rates ($\dot{B}_{input}$), a metric referred to as the degree of perfection (Kotas, 1985), as defined in Eq. (7):

$$\eta_{B,SOEC} = \frac{\dot{B}_{prod}}{\dot{B}_{input}} = \frac{\dot{B}_{H_2+H_2O,out} + \dot{B}_{O_2+H_2O,out}}{\dot{B}_{H_2O+H_2,in} + \dot{B}_{H_2O,in} + \dot{W}_{SOEC}} \tag{7}$$

The exergy efficiencies of the solar field, solar receiver, PV system, and heat exchangers HX-1 and HX-5 are defined as the ratio of output to input physical exergy rates. The compressors' exergy efficiencies were calculated based on the ratio of the change in exergy to the power supplied. The plant exergy efficiency is given by Equation (8):

$$\eta_{B,plant} = \frac{\dot{B}_{H_2,out} + \dot{B}_{O_2.out} + \dot{B}_{hotwater,out}}{\dot{B}_{PV,in} + \dot{B}_{CST,in}} \tag{8}$$

For the PV and CST systems, the input exergy rates are defined in terms of the energy rates (Petela, 2010), according to Equation (9), where T represents the temperature of the solar surface (5778 K), and T_0 denotes the ambient temperature (298 K).

$$\frac{\dot{B}_{SF/PV,in}}{\dot{E}_{SF/PV,in}} = 1 - \frac{4}{3}\frac{T_0}{T} + \frac{1}{3}\left(\frac{T_0}{T}\right)^4 \tag{9}$$

The thermoeconomic balance for each component of the plant is defined based on Equation (10) where $\dot{C}_{inp}$ and $\dot{C}_{prod}$ are the cost rates in \$/s associated with the inputs and products of the process, and $\dot{Z}$ is the capital cost rate, which includes expenses for system acquisition, operation, and maintenance (Tsatsaronis, 1993). This equation can be rewritten in terms of the unit exergy cost (c) in \$/kJ, according to Equation (11).

$$\dot{C}_{inp} + \dot{Z} = \dot{C}_{prod} \tag{10}$$

$$c_{inp} \cdot \dot{B}_{inp} + \dot{Z} = c_{prod} \cdot \dot{B}_{prod} \tag{11}$$

https://doi.org/10.52202/077185-0044

The cost rate of each component can be assessed from Equation (12), where Z is the total installation cost, f_{CR} is the capital recovery factor, is the $f_{O\&M}$ operating and maintenance factor, and N_h is the number of annual hours of plant operation. The capital recovery factor is determined in terms of the plant useful life and the investment interest rate.

$$\dot{Z} = \frac{Z \cdot f_{CR} \cdot f_{O\&M}}{3600 \cdot N_h} \tag{12}$$

Table 1 details the equations for calculating the PV, CST, and SOEC system installation costs.

Table 1: Cost equations

Component	Installation Costs Equations (USD)
PV system	$747 \cdot \dot{W}_{PV}$
Solar heliostat	$127 \cdot N_{heliostat} \cdot A_{heliostat}$
Solar tower	$3 \cdot 10^6 \cdot \exp(0.0113 \cdot z_{tower})$
Solar receiver	$103 \cdot 10^6 \left(\frac{A_{receiver}}{1571}\right)^{0.7}$
Thermal tanks	$79200 \cdot E_{storage}$
SOEC module	$1500 \cdot \dot{W}_{SOEC}$

Sources: Böhm et al. (2020), IRENA (2023), and NREL (2023).

The methodology presented by Turton et al. (2012) was applied to estimate the costs (Z) of the other components. It considers the Module Costing Technique (MCT) to calculate the investment costs for an industrial plant project. The component cost can be estimated using Equation (13). Here, C_P is the purchased cost of the component for base conditions. The factors f_{af}, f_{cont}, and f_{fee} are related to the auxiliary facilities, contingency, and fees, respectively. The bare module factor, f_{BM}, depends on the material the component is made of and its operating pressure.

$$Z = f_{af} C_P + (1 + f_{cont} + f_{fee}) f_{BM} C_P \tag{13}$$

The purchased cost of each component was calculated using the cost equations in Table 1, which have been updated for 2022 using the Chemical Engineering Plant Cost Index (CEPCI).

Table 1: Cost equations

Component	Purchased Costs Equations (USD)
Evaporator (forced circulation)	$2.06 \cdot (10^{5.0238+0.3475 \log A+0.0703(\log A)^2})$
Heat exchangers (floating head)	$2.06 \cdot (10^{4.8306-0.8509 \log A+0.3187(\log A)^2})$
Heat exchangers (fixed tube)	$2.06 \cdot (10^{4.3247-0.3030 \log A-0.1634(\log A)^2})$
Pump (centrifugal)	$2.06 \cdot (10^{3.3892+0.0536 \log \dot{W}+0.1538(\log \dot{W})^2})$
Compressors (rotary)	$2.06 \cdot (10^{5.0355-1.8002 \log \dot{W}+0.8253(\log \dot{W})^2})$

Sources: Turton et al. (2012)

In addition to the 2022 scenario, costs were evaluated for the mid-term (2030) and long-term (2050) scenarios. For this purpose, the PV, CST, and SOEC systems costs were estimated according to the

https://doi.org/10.52202/077185-0044

percentages listed in Table 2, which are expressed relative to current costs. A significant cost reduction is anticipated for SOEC cells as the technology matures and scales up.

Table 2: Scenarios for thermoeconomic analysis

Scenario	PV	CST	SOEC
2030	80%	80%	33%
2050	65%	65%	18%

Sources: Böhm et al. (2020) and DNV (2023).

Finally, calculating all cost rates and applying the thermoeconomic balance to each plant component can determine the levelized cost of hydrogen (LCOH) in $/kg using Equation (14) regarding its unit cost and the specific exergy.

$$LCOH = c_{H2} \cdot b_{H2} \tag{14}$$

3 RESULTS AND DISCUSSION

3.1 Model Validation

The system model validation has been completed using data from Hauch et al. (2020) regarding electrolyzers manufactured in 2006 and 2020, as shown in Fig. 2. This graph displays the polarization curve of the cells, with model accuracy improving as the voltage nears the thermoneutral value.

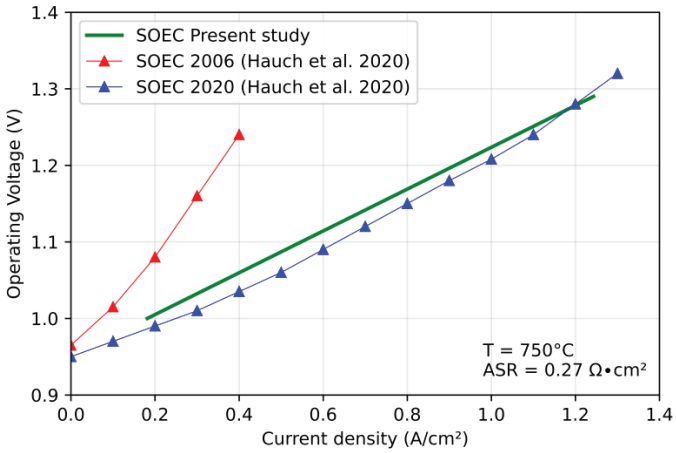

Figure 2: Data for model validation

3.2 Electricity generation and hydrogen production

Table 3 presents the main results for the analyzed plant. With thermal storage, the plant can operate for an average of 14 hours daily, resulting in a capacity factor of 52.7% for H_2 production. A 292 MW photovoltaic system is required to meet the electricity demand.

Figure 3(a) presents the daily electricity generation and demand curves, while Figure 2(b) illustrates these curves over the year. During daylight hours, the plant's energy needs are met by photovoltaic generation, with surplus electricity being exported to the grid for nighttime use. Annually, 42.7% of the electricity utilized by the plant comes from the grid. Different strategies can be considered to reduce dependence on grid usage. One option would be to include a battery bank in the plant, which would significantly increase the cost of hydrogen production. Reducing the hours of thermal storage is another alternative. However, this might lead to a lower capacity factor and increased thermal fluctuations and

https://doi.org/10.52202/077185-0044

stresses in the electrolyzers, potentially reducing plant efficiency due to prolonged operation in a transient state. Finally, implementing a hybrid generation plant combining wind and photovoltaic systems could help balance the plant's energy demand throughout the year and minimize seasonal storage needs. Selecting any strategy requires a comprehensive analysis of technical and economic factors to ensure optimal plant operation.

Table 3: Operational results for SOEC, CST, and PV systems

Parameter	Value
SOEC	
Capacity factor (%)	52.7
Full load utilization (%)	44.9
Mean daily operating hours (h)	14.0
Annual electricity demand (GWh)	471.1
CST	
Number of heliostats	886
Mean solar field optical efficiency (%)	55.4
Mean receiver thermal efficiency (%)	90.1
Thermal power output at design point (MW)	26.2
Annual thermal energy output (GWh)	123.3
PV	
Nominal capacity (MW)	292.0
Capacity factor (%)	20.3
Annual electricity production (GWh)	518.5
Electricity delivered to the grid (%)	42.7

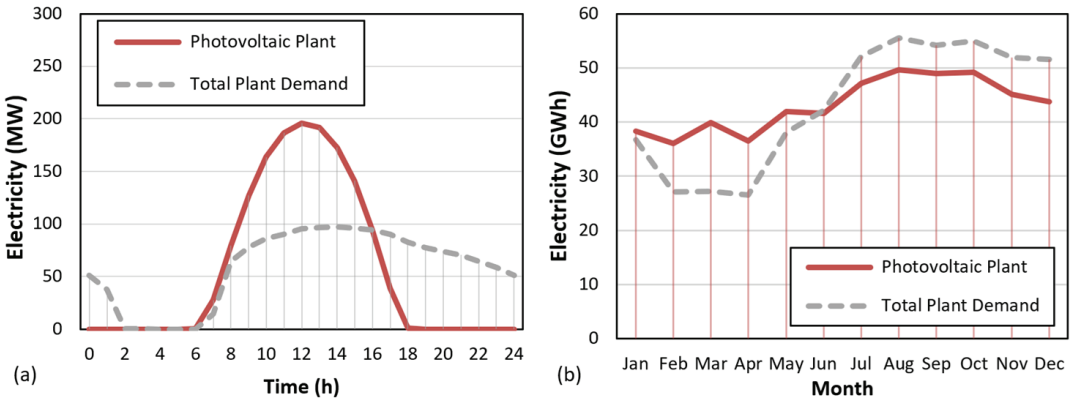

Figure 3: Electricity generation and demand: (a) daily average profile (b) monthly values for a TMY

Figs. 4(a) and 4(b) present the average daily hydrogen production curve and the estimated monthly hydrogen production. The average daily production is estimated to be 36.6 t, resulting in 290.8 t of oxygen and a water consumption rate of approximately 328.4 m³/day in the electrolyzers. Monthly, the

https://doi.org/10.52202/077185-0044

production averages 1114.4 t of hydrogen. However, production in April is less than half of that in August, mainly due to variations in direct solar radiation affected by rainfall patterns. Throughout the year, the monthly capacity factor of the SOEC system ranges from 32.2% to 64.3%.

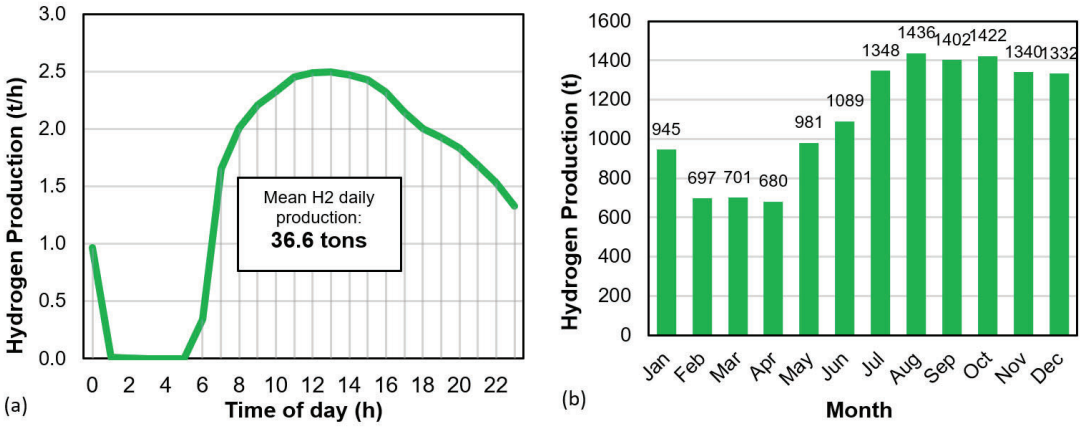

Figure 4: Hydrogen production: (a) daily average profile and (b) monthly values for a TMY

3.3 Exergy evaluation

Table 4 summarizes the exergy analysis results considering operation at a steady state.

Table 4: Results of the exergy analysis

Components	Exergy destruction (MW)	Exergy Efficiency (%)
Photovoltaic System	520.12	17.3
Solar Field	21.75	55.4
Solar Receiver	12.07	55.3
Electrolyzer (SOEC)	8.39	93.8
H_2 compressors	1.05	83.9
O_2 compressors	0.34	84.0
Electric heater	0.16	66.9
Pump	0.03	80.7
Evaporator	6.01	59.8
Recuperator 1	0.25	95.5
H_2/H_2O Coolers	0.64	64.8
H_2 Intercoolers	0.35	58.2
Recuperator 2	0.23	95.3
O_2/H_2O Coolers	1.22	56.9
O_2 Intercoolers[(1)]	0.14	56.7
Other components	1.25	-
Total	574.0	15.6

https://doi.org/10.52202/077185-0044

In the PV system, heliostats, and receiver, there are optical losses such as attenuation, blocking, or shadowing, in addition to heat convection and conduction losses. The PV system accounts for 90.6% of the plant's exergy destruction, and the CST components represent 5.9%. Notably, the solar receiver's exergy efficiency is lower than that of other heat exchangers, indicating the irreversibility associated with converting solar radiation into the physical exergy of solar salt.

The SOEC stacks presented a high exergy efficiency of 93.8%, demonstrating the advantage of operating at high temperatures. The primary sources of irreversibility in the electrolyzers are overvoltage at the anode and cathode and ohmic resistance within the cells. The total electricity consumption of the operational modules is 100 MW, accounting for 91.6% of the plant's total electricity consumption. The evaporator operates at 59.8% efficiency, while the recuperators exceed 95% efficiency due to better thermal matching and no phase change. The coolers have slightly reduced efficiency due to steam condensation. Overall, the heat exchangers between the electrolyzers and separators have a total exergy efficiency of 80.3%, recovering 23.4 MW of exergy and reducing the need for additional external solar exergy input. The intercoolers' exergy efficiency is based on the recovered exergy, with 1.90 MW of physical exergy that can be reused for facility applications, such as powering an absorption refrigeration cycle or driving an organic Rankine cycle to generate additional electricity. Finally, the total exergy efficiency obtained for the plant is 15.6%. Figure 5 details the contribution of each input and product to achieve this efficiency.

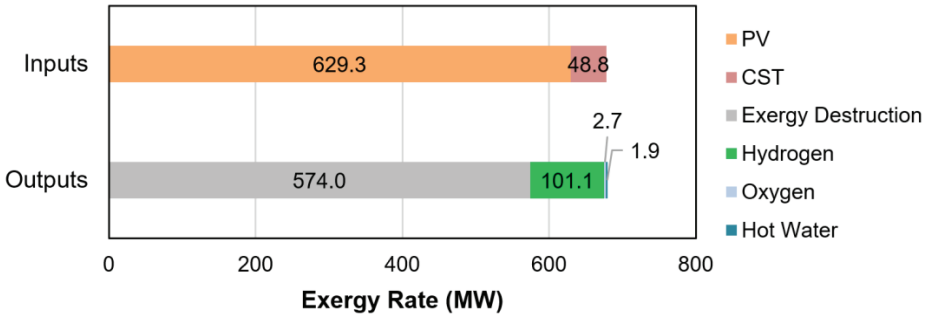

Figure 5: Exergy rates of inputs and products

3.4 Thermoeconomic Analysis

Three scenarios – 2022, 2030, and 2050 – were considered to determine the costs of each component. In the 2022 scenario, the total installation cost of the plant was estimated to be 486 million dollars. Figure 6 illustrates the cost breakdown for each component. The PV system and SOEC modules account for 75% of the total cost.

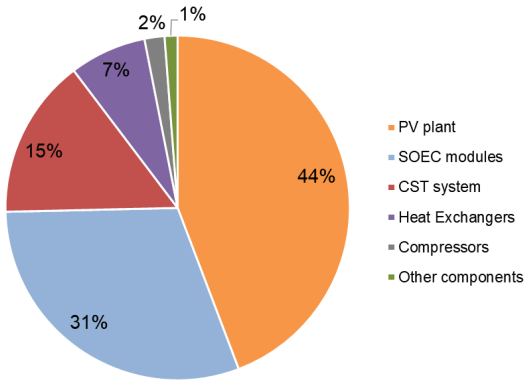

Figure 6: Fraction of the total module cost per component (2022)

https://doi.org/10.52202/077185-0044

The cost rates were estimated considering f_{ac}, f_{cont}, and f_{fee} equal to 0.50, 0.18, and 0.03, respectively. The analysis also assumed a 20-year lifespan for the plant, a 15% interest rate, and an O&M factor of 1.03. Based on these parameters, the LCOH for hydrogen was estimated for the three conditions considered, as illustrated in Figure 7.

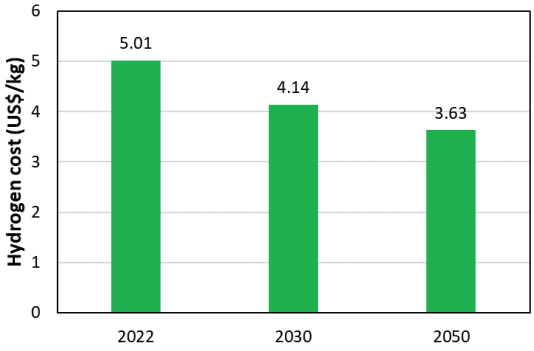

Figure 7: Hydrogen production cost

The cost of 5.01 USD/kg is within the range of costs reported by the International Energy Agency (2023) for electrolysis with solar energy, as well as the cost estimated for 2030. While these costs are higher than those for non-renewable hydrogen production methods (1.00-3.00 USD/kg), it is essential to note that this comparison overlooks the environmental and greenhouse gas emissions costs associated with fossil fuel-based hydrogen. Despite its higher initial cost, green hydrogen presents a more sustainable solution in the long term. Additionally, the plant generates oxygen at a competitive cost of 0.02 USD/kg across all scenarios, providing an additional source of revenue. Cost reductions can be achieved by decreasing component expenses and through operational optimizations, such as extending operational hours and enhancing the plant's capacity factor. Furthermore, integrating energy storage systems and intelligent energy management can improve the efficiency of renewable energy usage, leading to lower operational costs and making green hydrogen an increasingly competitive alternative.

4 CONCLUSIONS

This study conducted an exergy and thermoeconomic evaluation of a novel configuration for a solar-powered high-temperature electrolysis plant for hydrogen production. The facility was designed with a capacity of 100 MW-SOEC, comprising 20 modules of 5 MW each. The analysis focused on the northeast coast of Brazil, using a photovoltaic system for electricity supply and a concentrated solar thermal system with thermal energy storage for steam generation. The plant can operate for an average of 14 hours per day, achieving a capacity factor of 52.7%, with an estimated daily production of 36.6 t of hydrogen. The exergy efficiency of the proposed plant is 15.6%, with SOEC stacks exhibiting a high exergy efficiency of 93.8%, underscoring the benefits of high-temperature operation. Finally, the levelized cost of hydrogen (LCOH) is estimated at 3.63 USD/kg for a long-term scenario.

It is essential to highlight that the exergy used in the evaluated configuration is entirely obtained from a renewable resource, with no direct CO_2 emissions. This offers a significant advantage over conventional hydrogen production methods. Although still in the research and development phase, SOEC technology holds promise as an alternative for hydrogen production, with the potential for further efficiency improvements and cost reductions. The anticipated cost reductions for photovoltaic and concentrated solar thermal systems also indicate a promising future for this integration, with a substantial decrease in LCOH expected. Moreover, the study identifies opportunities for enhancements, such as extending operational hours and integrating with wind energy. Overall, this research provides valuable insights into the technical and economic feasibility of solar-driven high-temperature electrolysis for hydrogen production, contributing to developing sustainable energy solutions.

https://doi.org/10.52202/077185-0044

NOMENCLATURE

Latin letters

A	area (m²)
ASR	area specific resistance (Ω·cm²)
b	specific exergy (kJ/kg)
B	exergy (kJ)
Ḃ	exergy flow rate (kW)
c	unit cost ($/kJ)
Ċ	cost rate ($/s)
E	energy (kJ)
Ė	energy rate (kW)
f	factor
F	Faraday constant (96,486 C/mol)
G	Gibbs free energy (kJ)
H	enthalpy (kJ)
j	current density (A/cm²)
p	pressure (bar)
V	voltage (V)
Ẇ	power (kW)
m	mass (kg)
ṁ	mass flow rate (kg/s)
N	quantity
ṅ	molar flow rate (kmol/s)
R	universal gas constant 8.314 kJ/kmol·K
S	entropy (kJ/K)
T	temperature (K)
z	height (m)
Z	capital cost ($)
Ż	capital cost rate ($/s)

Greek symbols

Δ	variation
ε	resistance coefficient
η	efficiency

Subscripts and superscripts

0	standard
af	auxiliary facilities
b	exergy
BM	bare module
cont	contingency
CR	capital recovery
CST	concentrating solar thermal
inp	input
min	minimum
N	Nerst
O&M	operating and maintenance
P	purchased
prod	products
PV	photovoltaic system
SOEC	solid oxide electrolysis cells
TN	thermoneutral

REFERENCES

Abdin, Zainul et al. 2020. "Hydrogen as an Energy Vector." *Renewable and Sustainable Energy Reviews* 120(November 2019).

Bell, Ian H, Jorrit Wronski, Sylvain Quoilin, and Vincent Lemort. 2014. "Pure and Pseudo-Pure Fluid Thermophysical Property Evaluation and the Open-Source Thermophysical Property Library Coolprop." *Industrial and Engineering Chemistry Research* 53(6): 2498–2508.

Böhm, Hans, Andreas Zauner, Daniel C. Rosenfeld, and Robert Tichler. 2020. "Projecting Cost Development for Future Large-Scale Power-to-Gas Implementations by Scaling Effects." *Applied Energy* 264(February): 114780. https://doi.org/10.1016/j.apenergy.2020.114780.

Capurso, T., M. Stefanizzi, M. Torresi, and S.M. Camporeale. 2022. "Perspective of the Role of Hydrogen in the 21st Century Energy Transition." *Energy Conversion and Management* 251(November 2021): 114898. https://doi.org/10.1016/j.enconman.2021.114898.

DNV. 2023. Dnv *Energy Transtion Outlook: A Global and Regional Forecast to 2050*. Hovik, Norway. https://www.dnv.com/energy-transition-outlook/index.html.

Fu, Qingxi et al. 2010. "Syngas Production via High-Temperature Steam/CO2 Co-Electrolysis: An Economic Assessment." *Energy and Environmental Science* 3(10): 1382–97.

Hansen, John Bøgild. 2015. "Solid Oxide Electrolysis - a Key Enabling Technology for Sustainable Energy Scenarios." *Faraday Discussions* 182: 9–48. http://dx.doi.org/10.1039/C5FD90071A.

Hauch, A. et al. 2020. "Recent Advances in Solid Oxide Cell Technology for Electrolysis." *Science* 370(6513).

IEA. 2023. "Global Hydrogen Review 2023." *Global Hydrogen Review 2023*.

IRENA. 2023. "Renewable Generation Costs in 2022." *International Renewable Energy Agency*: 69.

Kotas, T. J. 1985. Journal of Mechanical Working Technology *The Exergy Method of Thermal Plant*

https://doi.org/10.52202/077185-0044

Analysis. London: Butterworths.
Mohebali Nejadian, Mehrnaz, Pouria Ahmadi, and Ehsan Houshfar. 2023. "Comparative Optimization Study of Three Novel Integrated Hydrogen Production Systems with SOEC, PEM, and Alkaline Electrolyzer." *Fuel* 336(November 2022): 126835. https://doi.org/10.1016/j.fuel.2022.126835.
NREL, National Renewable Energy Laboratory. "PySAM." sam.nrel.gov/software-development-kit-sdk/pysam.html.
O'Brien, James E. 2012. "Thermodynamics and Transport Phenomena in High Temperature Steam Electrolysis Cells." *Journal of Heat Transfer* 134(3): 1–11.
Petela, Ryszard. 2010. *Engineering Thermodynamics of Thermal Radiation For Solar Power Utilization*. New York: McGraw Hill.
Petipas, Floriane, Annabelle Brisse, and Chakib Bouallou. 2013. "Model-Based Behaviour of a High Temperature Electrolyser System Operated at Various Loads." *Journal of Power Sources* 239(2013): 584–95. http://dx.doi.org/10.1016/j.jpowsour.2013.03.027.
Pourasl, Hamed H., Reza Vatankhah Barenji, and Vahid M. Khojastehnezhad. 2023. "Solar Energy Status in the World: A Comprehensive Review." *Energy Reports* 10(October): 3474–93. https://doi.org/10.1016/j.egyr.2023.10.022.
Restrepo, Julián C. et al. 2022. "Techno-Economical Evaluation of Renewable Hydrogen Production through Concentrated Solar Energy." *Energy Conversion and Management* 258: 115372. https://linkinghub.elsevier.com/retrieve/pii/S0196890422001686.
Sengupta, Manajit et al. 2018. "The National Solar Radiation Data Base (NSRDB)." *Renewable and Sustainable Energy Reviews* 89(March): 51–60. https://doi.org/10.1016/j.rser.2018.03.003.
Squadrito, Gaetano, Gaetano Maggio, and Agatino Nicita. 2023. "The Green Hydrogen Revolution." *Renewable Energy* 216(March): 119041. https://doi.org/10.1016/j.renene.2023.119041.
Tsatsaronis, George. 1993. "Thermoeconomic Analysis and Optimization of Energy Systems." *Progress in Energy and Combustion Science* 19(3): 227–57.
Turton, Richard et al. 2012. *Analysis , Synthesis , and Design of Chemical Processes Fourth Edition*. 4th ed. Saddle River, New Jersey: Prentice Hall.
Younas, Muhammad et al. 2022. "An Overview of Hydrogen Production: Current Status, Potential, and Challenges." *Fuel* 316(December 2021): 123317. https://doi.org/10.1016/j.fuel.2022.123317.

ACKNOWLEDGEMENT

The first author acknowledges the Federal Institute of Education, Science and Technology of Minas Gerais (IFMG) – Campus Formiga for its support during the development of this study. The second author acknowledges CNPq (National Council for Scientific and Technological Development) for grant 306484/2020-0.

https://doi.org/10.52202/077185-0044